COMPDYN 2011
III ECCOMAS Thematic Conference on
Computational Methods in Structural Dynamics and Earthquake Engineering
M. Papadrakakis, M. Fragiadakis, V. Plevris (eds.)
Corfu, Greece, 25–28 May 2011

SEISMIC EVALUATION OF EXISTING BASEMENT WALLS

Alireza Ahmadnia, Mahdi Taiebat, W.D. Liam Finn, and Carlos E. Ventura

Department of Civil Engineering, University of British Columbia, Vancouver, BC, Canada
(ahmadnia, mtaiebat, finn, ventura)@civil.ubc.ca

Keywords: Basement wall, seismic, lateral earth pressure.

Abstract. *Structural and geotechnical engineers have long relied upon the use of the popular Mononobe-Okabe (M-O) method for determining seismic lateral pressures acting on retaining walls. This limit equilibrium-based method was originally developed for rigid retaining walls with sufficient rigid body displacements to mobilize the active wedge in the backfill soil. In reality, however, certain types of retaining walls, such as basement walls, have variable degrees of flexibility and deformation at different depths. Recently, the Structural Engineers Association of British Columbia (SEABC) initiated a task force to review the problem. The authors are members of this task force committee and have carried out series of dynamic numerical analyses to study lateral earth pressures against basement walls taking into account the flexibility and potential yielding of the wall components. This paper outlines a part of the findings in this study.*

1 INTRODUCTION

Basement walls constitute an integral part of tall buildings. These walls should be designed to resist the static and seismically induced lateral earth pressures. Since no guideline exists that specifically addresses seismic design of basement walls, designers use the Coulomb theory to find the static active lateral thrust from soil to the wall and the Mononobe and Okabe (M-O) method [1] to find the total (static and earthquake induced) active lateral thrust during seismic loading. Based on the Coulomb theory and the M-O method the active static and the total (static and earthquake induced) active lateral thrusts on a wall are given by $P_A = \gamma H^2 K_A / 2$ and $P_{AE} = \gamma H^2 K_{AE} / 2$, respectively, where P_A and P_{AE} are the active earth pressure coefficient without and with the earthquake effect, γ is the soil density, and H is the retaining wall height. For a straight wall with level backfill, K_A and K_{AE} are mainly functions of the friction angle of the soil and the angle of wall friction. The K_{AE} is also a function of the horizontal and vertical coefficients of Peak Ground Acceleration (PGA). These limit equilibrium-based methods were originally developed for rigid retaining walls with sufficient rigid body displacements to mobilize the active wedge in the backfill soil. Basement walls, on the other hand, have variable degrees of flexibility and deformation at different depths. The M-O method also assumes that the movement of basement wall will be sufficient to produce minimum active pressure. It also assumes that the soil behind the wall acts as a rigid body and does not account for flexibility of the soil-structure system. The M-O method only provides the total lateral earth pressure, P_{AE}. It does not explicitly indicate anything about the distribution of lateral earth pressure from seismic events. Several studies have been conducted for investigating the distribution of the lateral earth pressures and the point of application of the resultant lateral forces, depending on the mode of deformation of the wall (e.g., see [2–4]).

The current state of practice for design of basement walls is using the Coulomb theory and the M-O method for finding the static and total lateral thrusts, P_A and P_{AE}. It is also the current state of practice to use the PGA for application of the M-O method in the basement wall problems. In this method the soil is assumed to behave as a rigid mass and consequently the inertial force is equally distributed throughout the soil mass. However, wave scattering analyses by Segrestin and Bastick [5] show that for walls in excess of 20 or 30 ft, it is more justified to use an equivalent seismic coefficient. AASHTO LRFD Bridge Design Specification [6] provides a useful guideline for the conventional gravity and semi-gravity cantilever walls, non-gravity walls, and anchor walls. The guideline suggests the use of M-O method to estimate equivalent static force for gravity walls. However for non-gravity walls the guideline is not explicit and suggests the use of the M-O method with a factor for adjusting the PGA as a function of the wall height. For finding the distribution of the total lateral thrust, the P_A is distributed linearly along the wall height as a triangle with zero pressure at the surface and a pressure equivalent to $\gamma H K_A$ at the base. The total active thrust can be divided into the static component, P_A, and a dynamic component $\Delta P_{AE} = P_{AE} - P_A$. It is the current state of practice to distribute the dynamic component ΔP_{AE} as an inverse triangle along the height of the wall with zero pressure at the base of the wall and a pressure equivalent to $\gamma H(K_{AE} - K_A)$ at the ground surface. This distribution of lateral earth pressures is then used for finding the resulting moments in the walls and eventually simplified design of the walls.

The seismic hazard level in the 1995 edition of the National Building Code of Canada [7] for design of buildings had a probability of exceedance of 10% in 50 years. The related PGA hazard under NBCC1995 is 0.24g for Vancouver area. The designers were using the M-O method, as explained above, with this PGA for estimating the seismic lateral pressures and eventually designing the basement walls. The 2005 edition of the National Building Code of Canada [8] suggest a higher seismic hazard level for design of buildings that is probability of

exceedance of 2% in 50 years. For Vancouver, the related PGA hazard under NBCC2005 is as big as 0.46g. Using the M-O method with this high PGA results in a high demand in designing the basement walls and this has raised some concerns for the design engineers on the applicability of the M-O method for the basement walls.

Recently, the Structural Engineers Association of British Columbia (SEABC) initiated a task force to review the problem. The authors are members of this task force committee and have carried out series of dynamic numerical analyses that take into account the flexibility and potential yielding of the wall components, as an effective procedure to study the lateral earth pressures against basement walls. To this end a specific type of wall, designed by the structural engineers using the current state of practice to withstand a seismic event in Vancouver with 10% probability of exceedance in 50 years, has been numerically analyzed in this study. Performance of this wall has been studied for three seismic events with 2% probability of occurrence in 50 years in Vancouver, a higher seismic demand enforced by the NBCC2005. In addition, the dynamic analysis results are compared to the standard methods of determining lateral earth pressures on the wall. The results to date indicate that flexibility of the walls has important effects on the distribution of the seismic lateral pressures on the walls. This paper outlines a part of the findings in this study.

2 PROPERTIES OF WALL

A specific basement wall designed by the structural engineers for this study based on the current state of practice, as explained in the previous section. A PGA of 0.24g was used in M-O equation for design of the wall. This corresponds to a probability of exceedance of 10% in 50 years (NBCC1995), although the current PGA for design is 0.46g (NBCC 2005).

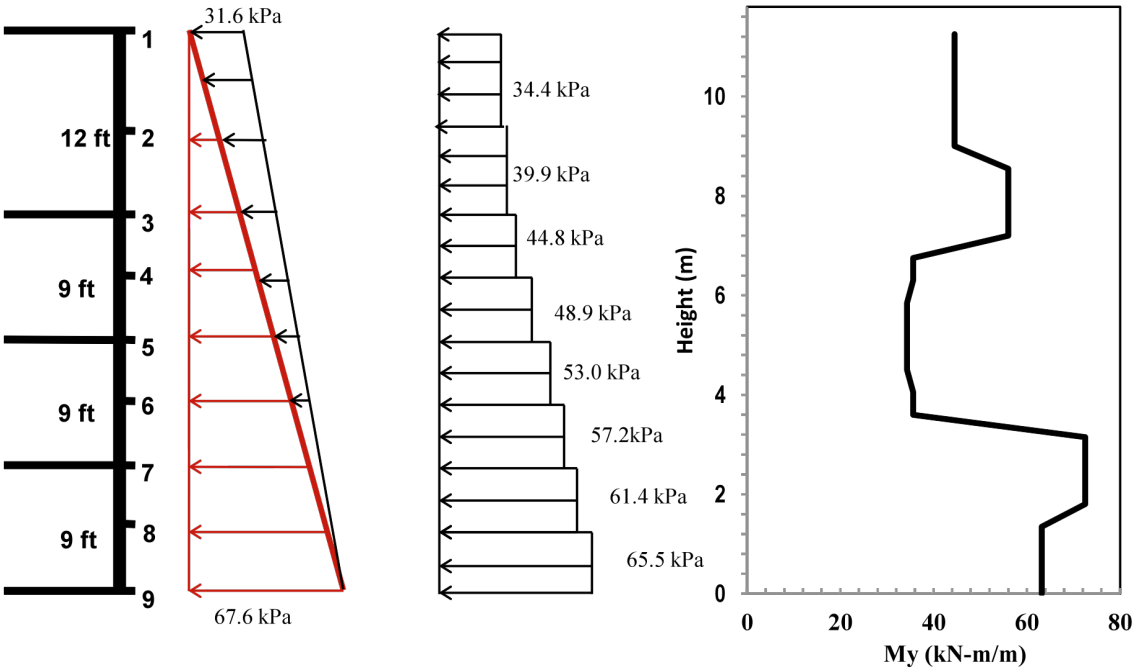

(a) (b)

Figure 1: (a) Distribution of the design lateral pressure along the height of the wall for based on the current state of practice for a seismic event with PGA=0.24g and a backfill soil with friction angle of 33°; (b) Resulting designed moment resistance distribution along the height of the wall.

The structural engineers were interested in how the basement wall designs based on the 1995 standard would behave under the 2005 loading. Figure 1(a) depicts the design lateral earth pressure distribution for the basement wall for a friction angle of 33 degrees and seismic coefficient of PGA=0.24g. The required moment resistance of the wall is the calculated along its height, as shown in Fig. 1(b), based the distributed pressures on the wall. In this design the structural engineer has not used any load reduction factor or ductility factor for the applied pressures on the wall. Uniform properties of I= 0.0013 m^4, A=0.25 m^2, and E=2.74×10^7 kN/m^2 are considered along the height of the basement wall.

3 DESCRIPTION OF THE MODEL

3.1 Model building

Non-linear seismic response of the basement wall is analyzed by using the two-dimensional finite difference computer program FLAC 6.00 [9]. Different stages of the modeling procedure are presented in Fig. 2. In order to ensure the proper initial stress distribution on the basement the actual construction sequence is modeled. First, a 24.3 m deep and 150 m wide layer of soil is created and brought to equilibrium under gravity forces. The model consists of two soil layers that will be discussed further in the next section. A part of the upper soil layer is then excavated in lifts to a depth of 11.7 m and a width 30m as shown in Fig. 2(a). As each lift was excavated, lateral pressures (shoring) are applied to retain the soil. Then as depicted in Fig. 2(b) the basement wall is constructed and global equilibrium is re-established. In the next stage, as shown in Fig. 2(c), the shoring pressures are removed, and load from the soil is transferred to the basement wall. The flexural behavior of the walls is modeled by elastic-perfectly plastic beam model with yield moments equal to the corresponding moment resistance values as shown in Fig. 1(b).

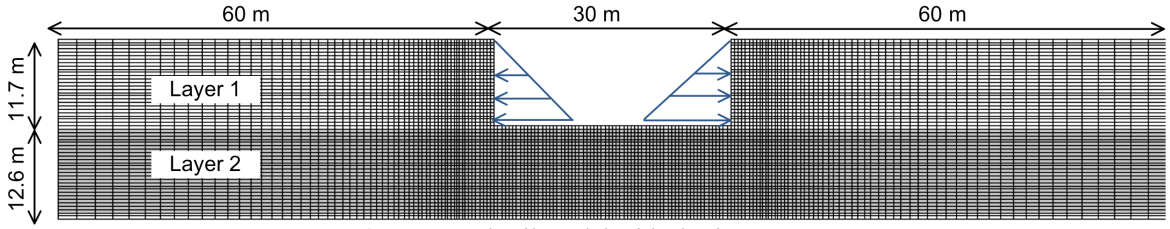

a) Excavated soil model with shoring pressures

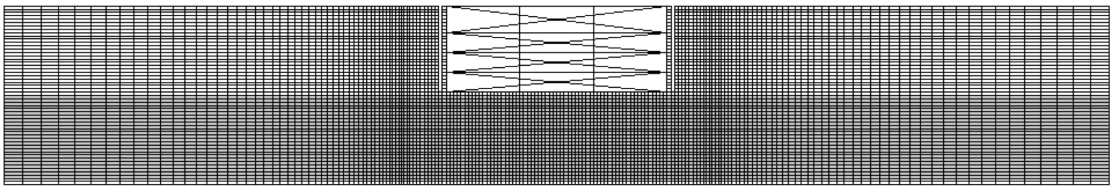

b) Construction of basement walls

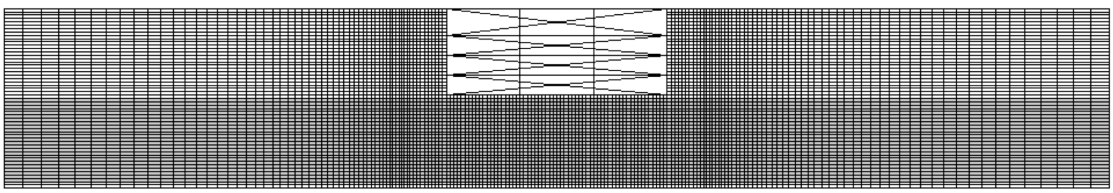

c) Removing shoring pressures, and applying the earthquake

Figure 2: Different stages of modeling procedure in FLAC.

3.2 Properties of soil

Constitutive response of the soil is modeled by a Mohr-Coulomb material model. The required model parameters are elastic bulk and shear moduli, cohesion, and friction and dilation angles of soil. The properties used in conjunction with the Mohr-Coulomb model for layers 1 and 2 of soil, as depicted in Figure 1, are presented in Table 1. Based on the results of a Shake analysis [10] for the present soil profile, the selected ground motions in this study, and a representative modulus reduction curve for the soil, an equivalent shear modulus equal to 30% of elastic shear modulus, i.e. G=0.3 G_{max}, was adopted for analysis.

Soil layer	Density (kg/m^3)	Bulk modulus (kPa)	G_{max} (kPa)	G/G_{max}	Cohesion (kPa)	Friction angle (degrees)	Dilations angle (degrees)
1	1950	1×10^5	5×10^4	0.3	0	33	0
2	1950	1×10^5	5×10^4	0.3	20	40	0

Table 1: Example of the construction of one table.

3.3 Ground motions

Ground motions for the analyses are selected from Pacific Earthquake Engineering Research (PEER) strong ground motion database. Based on the results of de-aggregation of the NBCC Uniform Hazard Spectrum (UHS), site class C for Vancouver, candidate input motions are selected in the magnitude range M=6.5–7.5 and the distance range 10–30 km using the program Design Ground Motion Library, DGML [11]. Table 2 shows the list of three ground motions selected for this study.

Ground motion	NGA #	Event	Year	Station	Magnitude
G1	162	Imperial Valley	1979	Calexico Fire	6.53
G2	987	Northridge	1994	LA-Centinela	6.69
G3	778	Loma Prieta	1989	Hollister	6.93

Table 2: List of selected ground motions.

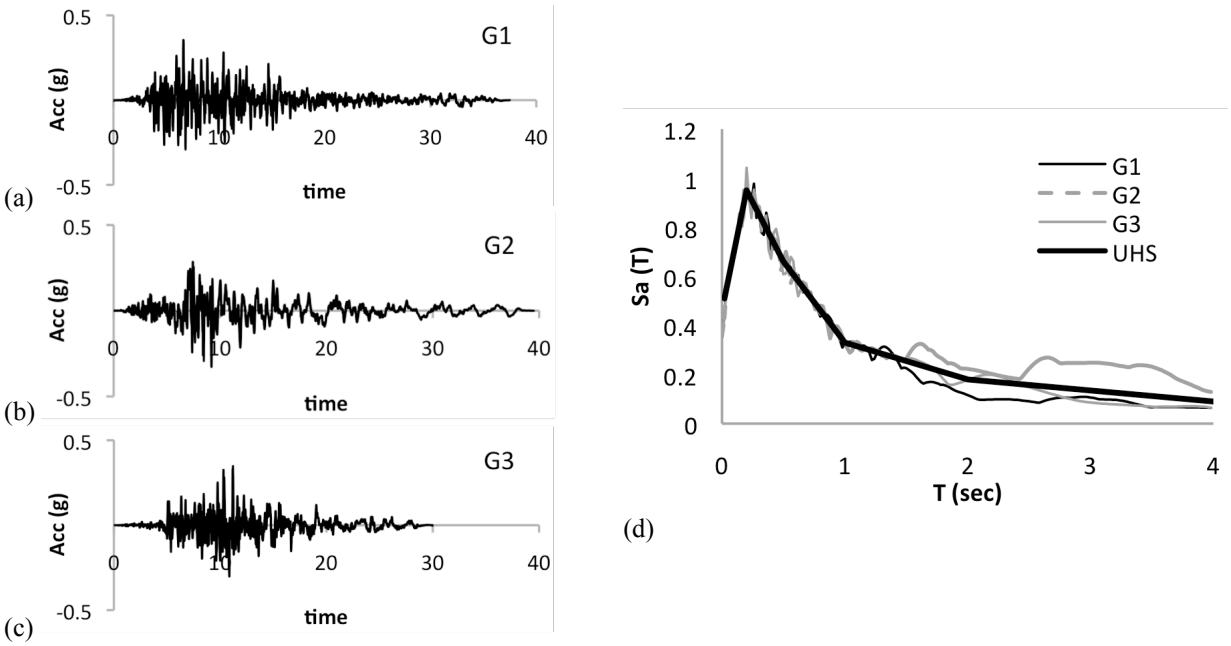

Figure 3: Time histories (a–c) and response spectra (d) of ground motions G1–G3 spectrally matched to UHS in periods 0.02–1.7 sec.

The selected ground motions are linearly scaled to match UHS using the computer program DGML and then spectrally matched to UHS in the period range of 0.02–1.7 sec, as shown in Fig. 3, using computer program SeismoMatch [12]. Figures 3(a-c) show the acceleration time histories of the three spectrally match ground motions and Fig. 3(d) shows the resulting response spectra compared to the UHS.

4 RESULT OF ANALYSIS

Numerical studies are conducted to evaluate the seismic response of basement walls which were designed for a PGA=0.24g that corresponds to a probability of exceedance of 10% in 50 years. The main seismic response parameters of the conducted analyses are: (a) the magnitude and distribution of lateral earth pressures, (b) the resultant lateral forces and the corresponding centers of application of the resultant force, (c) the basement wall bending moment and shear envelopes, and (d) the basement wall deflection envelopes, residual deflections, and drift ratio envelopes. These results are presented and discussed in this section.

Figure 4 shows lateral earth pressure time histories at three different levels along the height of the basement wall due to earthquake G1. The larger amount of stress produced at point 3 is due the existence of the basement floor at this level. In each one of these three elevations the initial static lateral pressures (before the earthquake) are lower than the residual static lateral pressure (after the earthquake).

The resultant lateral earth force at each time is obtained by integrating the lateral stresses along the height of the basement wall at that time. In addition, the moment arm at each time is calculated to track the center of application of the resultant force. The values of the resultant lateral earth force and its center of application are calculated for each time to generate the corresponding time histories for these two quantities during the dynamic simulation.

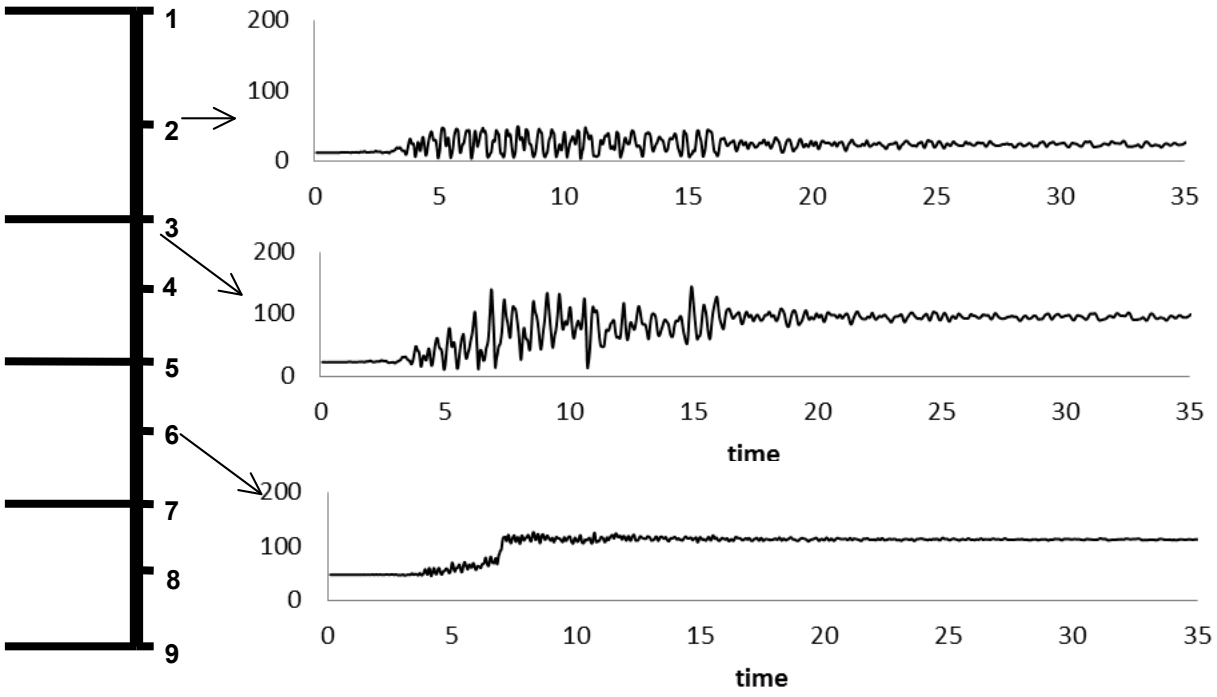

Figure 4: Numerical results of the lateral earth pressure time histories at different locations along the wall under ground motion G1.

Figure 5 shows the time histories of the resultant lateral earth force and the distance of its center of application from the base of the wall normalized with respect to the wall height (H) for three earthquakes. The corresponding results of a simplified method currently used in practice are also shown in this figure for comparison. In the simplified method, the resultant force (P_{AE}) is obtained by the M-O equation based on a design PGA level and the center of application of the resultant force is calculated assuming that the resulting ΔP_{AE} is applied approximately at a distance of 0.6H from the base of the wall. The simplified method is used for the hazard levels of PGA=0.24g (NBCC 1995), for which this wall is designed, and also for PGA=0.46g (NBCC 2005) which corresponds to the UHS that is used for spectral matching of the selected three ground motions in this study. Figures 5(a,c,e) show that the M-O method with PGA=0.46g reasonably predicts the maximum resultant force on the basement wall. Figures 5(b,d,f) show that with PGA=0.46g the simplified method for calculation of the center of application of the results force slightly over-predicts the elevation of the application center of the resultant lateral earth force on the wall at the instance of the maximum resultant force.

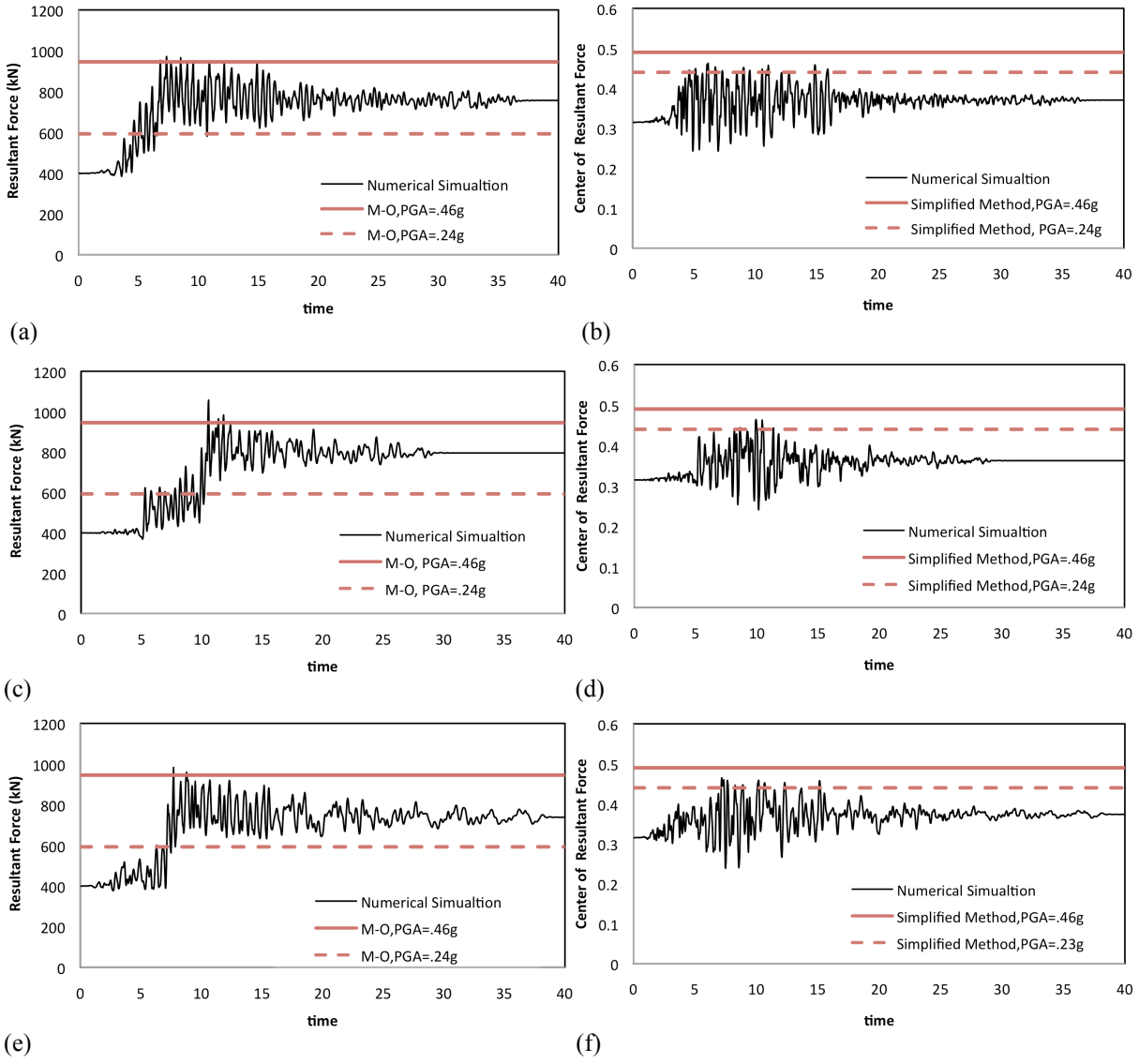

Figure 5: Time histories of the resultant lateral earth forces and the normalized center of the resultant forces for ground motions G1 (a,b), G2 (c,d), and G3 (e,f).

The dashed lines that correspond to the simplified method using PGA=0.24g are presented in Fig. 5 only as baselines for comparison.

Snapshots of the computed lateral earth pressure distribution along the height of the basement wall at different times are shown in Fig. 6. The results are for the analysis with ground motion G1. The results of numerical analysis are presented at four different times during the analysis. Figure 6(a) shows the analysis results at the beginning of dynamic analysis (symbols) and compares those to the suggested distribution of lateral pressures from Coulomb's theory (solid red line). The numerical analysis results at t=0 sec adequately match to those obtained from the Coulomb's theory for static lateral earth pressure distribution. Figures 6(b) and 6(c) present the numerical analysis results at t=7.7sec (the instance of occurrence of maximum lateral earth force on the wall) and t=10 sec (an arbitrary time during the shaking phase). These figures also show the suggested results from the simplified design procedure. By comparing the lateral earth pressures at t=7.7 sec or t=10 sec with the suggested distribution of the simplified method, it is evident that the simplified method cannot predict the lateral earth pressure adequately. The simplified method underestimates the lateral earth pressures at each floor slab level. In addition, for the most of the basement stories in this example, the simplified method overestimates the lateral earth pressures on the walls in between the floor slab levels. In other words, the numerical simulation results indicate that the lateral earth pressures are higher at the proximities of the floor slab locations (due to higher lateral stiffness of the floor slabs) and are lower on the mid height of the walls in between different floor levels (due to higher lateral stiffness of the walls compared to the slabs).

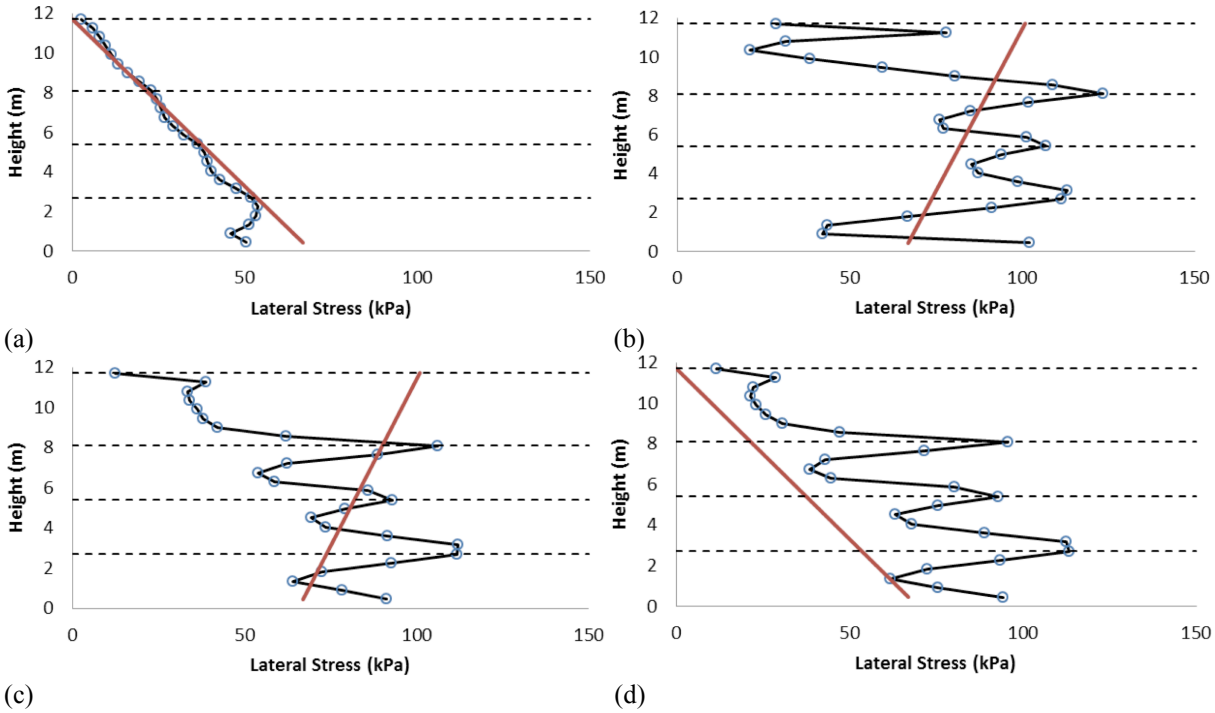

Figure 6: Lateral earth pressure distribution along the height of the basement wall for ground motion G1; symbols representing the results of numerical analysis at (a) t=0 sec (initial static pressures), (b) t=7.7 sec (the instance of occurrence of maximum lateral earth force on the wall), (c) t=10 sec (an arbitrary time during the shaking phase), and (d) t=42 sec (residual static pressures), and solid red lines representing the prediction from Coulomb's theory [for (a) and (d)] and the simplified design method [for (b) and (c)].

Finally Fig. 6(d) compares the numerical analysis results after the end of shaking (t=42 sec) with the suggested distribution of lateral pressures from Coulomb's theory. Numerical analysis results show a significant increase in the residual static earth pressure at the end of shaking. The significant difference between the two sets for distribution profiles of pressures can be attributed to the wall deformation.

The resulting bending moment and shear envelopes (maximum and minimum) over the wall height during the analysis with ground motion G1 are presented in Figs. 7(a) and 7(b), respectively. It is found that the resulting bending moment and shear envelopes for the three analyzed earthquakes are almost the same, and therefore only the analysis results of the basement wall subjected to ground motion G1 are shown here. In this figure, the limiting values of M_y and V_y correspond to nominal [designed] yield moment and yield shear of the wall sections, respectively. As shown in Fig. 7, the basement walls designed for a hazard level of 10% probability of exceedance in 50 years yields in moment at the mid-height of each basement story and also at each floor level. The shear diagram shows that the shear demand is considerably less than the shear capacity along the height of the wall.

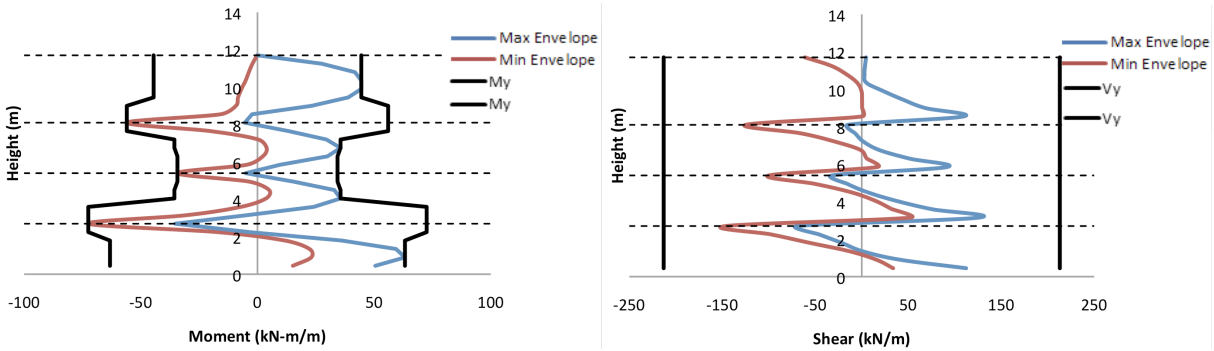

(a) (b)

Figure 7: The analysis results for bending moment and shear envelopes for the basement wall subjected to ground motion G1 and the nominal [designed] yield moments and yield shears of the basement wall.

Given that the wall yields at many different levels in the conducted analyses, it is very important to monitor the resulting deformations and drift ratios of the wall. The deformation or the relative displacement of the wall at each level is calculated as the difference between the displacement of the wall at that level and the displacement of the wall at its base. Drift ratio for each story is calculated as shown in Fig. 8. The resulting drift ratio from this figure is a useful indicator to determine the amount of damage to the wall. In this figure h_i is the floor height, $u_{\text{floor,top}}$ and $u_{\text{floor,bottom}}$ are the wall deformations at the floor levels and u_{wall} is the deformation at the mid height of the wall (between the two floors).

The envelopes of relative maximum and minimum displacements along with the residual relative displacements for the analysis with the three ground motions are shown in Fig. 9(a,c,e). The relative displacements are larger between the floors and are smaller at each floor level. The results of relative residual displacement show that the residual relative displacement of the wall at each floor level is approximately zero while in between different floor levels the wall shows some permanent deformations. The envelopes of drift ratios are shown in Figure 9(b,d,f). Maximum displacement and maximum drift ratio occur in the topmost story of the basement.

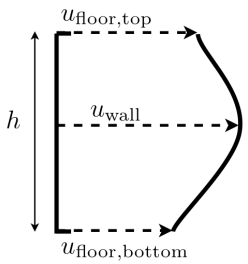

$$\text{Drift ratio} = \left[u_{\text{wall}} - \frac{u_{\text{floor,top}} + u_{\text{floor,bottom}}}{2}\right] / (0.5h)$$

Figure 8: Definition of drift ratio for each story of the basement wall.

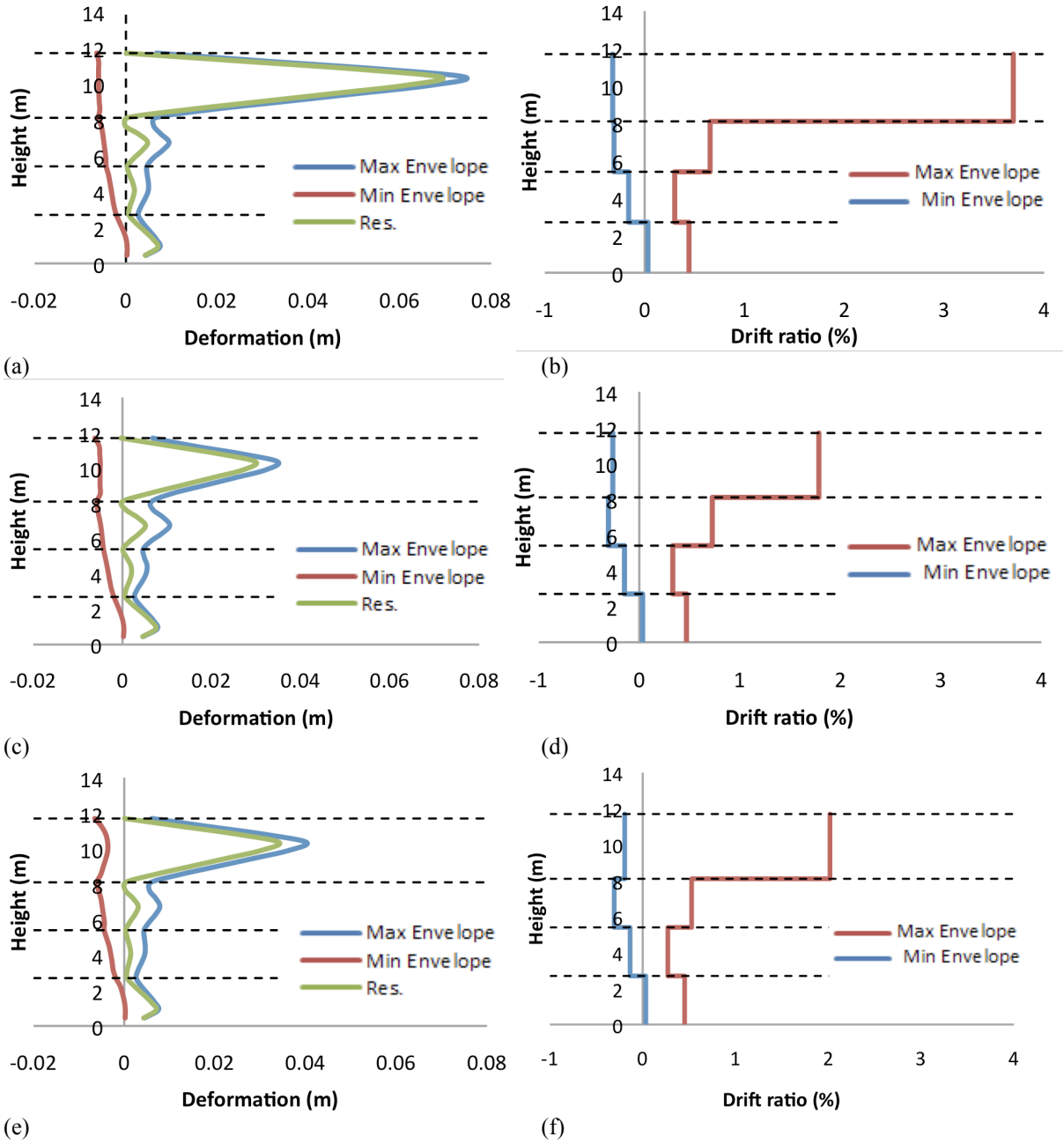

Figure 9: Envelops of maximum, envelopes of minimum, and values of residual wall deformations (displacements relative to the base of the basement wall) and envelop of maximum and envelopes of envelopes of minimum story drift ratios for ground motions G1 (a,b), G2 (c,d), and G3 (e,f).

5 SUMMARY AND CONCLUSION

One of the aims of this study was to assess whether existing basement walls designed for a hazard level with 10% probability of exceedance in 50 years (NBCC1995) in Vancouver would be safe when subjected to the higher seismic hazard level of 2% in 50 years which is mandated by the NBCC2005. The seismic pressures against the wall for design were calculated using the M-O procedure. The walls were designed to behave elastically under these pressures. The response of the walls to higher hazard level mandated by NBCC2005 was evaluated using the computer program FLAC.

The M-O pressures for the higher hazard are approximately double the pressures used for the original design. Therefore it was expected that the wall might yield under these elevated pressures and so a nonlinear analysis was carried out including nonlinear soil behavior and yielding of the wall. The analysis was conducted using three different input motions, all of them matched to Vancouver Uniform Hazard Spectrum in the period range 0.05–1.5 sec. The analyses show that M-O accurately predicts the peak resultant force on the wall and the point of application of the resultant force on the wall is consistently at about 0.55H from the base of the wall. This is the location usually assumed in British Columbia for application of M-O resultant force. However, the pressure distribution from the dynamic analysis was radically different from the linear distribution typically assumed in the practice. The total pressure during the earthquake against the top basement level is much smaller than estimated by M-O. At the end of earthquake, the residual pressure are significantly greater the Coulomb's theory.

It was found in Fig. 7(a) that in all levels the wall yields roughly at mid elevation and also yields at the floor levels on the opposite side. The behavior under shear is shown in Fig. 7(b) and it is shown that the shear demand is considerably less than the shear capacity along the height of the wall.

Figure 9 shows the deformations that occur in the wall in terms of displacement relative to the base of the wall and also in terms of drift ratios. The maximum drift ratio in the first level is approximately 4% for one of the motions. For the other motions the drift ratio is 2% in the top level. For the lower three basement levels the drift ratio is less than 1%. These results suggest that apart from the results for motion G1 the drift ratios are in acceptable limits so the elastic design under the seismic hazard of 10% in 50 years is almost adequate to carry the higher hazard of 2% in 50 years, except possibly in the upper basement level. More detailed study on this topic is underway by the authors.

ACKNOWLEDGEMENT

The materials presented in this paper are part of an ongoing study conducted by the authors as members of a task force committee for evaluation of seismic pressure on basement walls; struck by the Structural Engineers Association of British Columbia (SEABC). The authors are grateful for many constructive discussions with the Chairman of the Committee, Dr. Ron DeVall, and the committee members, Ali Amini, Don Anderson, Michael Belfry, Peter Byrne, Mat Kokan, Jim Mutrie, Ernest Naesgaard, Rob Simpson, and Doug Wallis.

REFERENCES

[1] Mononobe, N., and Matsuo, H. (1929). On the Determination of Earth Pressures During Earthquakes, *Proceedings of World Engineering Conference*, 9, 176-182.

[2] Seed, H.B., and Whitman, R.V. (1970). Design of Earth Retaining Structure of Dynamic Loads, *Proceedings, Specialty Conference on Lateral Stresses in the Ground and Design of Earth Retaining Structure*, ASCE, 103-147.

[3] Sherif, M.A. , Ishibashi, I. , and Lee, C.D. (1982). Earth Pressure Against Rigid Retaining Walls, *Journal of the Geotechnical Engineering Division*, ASCE, 108, GT5, 679-696.

[4] Sherif, M.A., and Fang, Y. S. (1984). Dynamic Earth Pressure on Walls Rotating about Top, *Soil and Foundations*, 24, 4, 109-117.

[5] Segrestin, P. and Bastick M. L. (1988). "Seismic Design of Reinforced Earth Retaining Walls , The Contribution of Finite Element Analysis." *International Geotechnical Symposium on Theory and Practice of Earth Reinforcement*, Fukuoka, Japan, October.

[6] American Association for State Highway and Transportation Officials, AASHTO (2010). LRFD bridge design specification (5nd ed.), Washington D. C.

[7] NRCC (1995). National building code of Canada 1995. *Institute for Research in Construction, National Research Council of Canada*, Ottawa, Ont.

[8] NRCC (2005). National building code of Canada 2005. *Institute for Research in Construction, National Research Council of Canada*, Ottawa, Ont.

[9] Itasca Consulting Group, Inc. (2008). FLAC: Fast Lagrangian Analysis of Continua, User Manual, Version 6.0, Minneapolis.

[10] Idriss, I. M. and Sun, J. I. (1992). "User's Manual for SHAKE91, A computer Program for Conducting Equivalent Linear Seismic Response Analyses of Horizontally Layered Soil Deposits Program Modified based on the Original SHAKE Program Published in December 1972 by Schnabel, Lysmer and Seed."

[11] SeismoMatch 1.0.3, Educational Version, SeismoSoft Company.

[12] Wang G., Power M., and Youngs R. (2009). Design Ground Motion Library (DGML), AMEC Geomatrix, Inc., Oakland, California, Project 10607.000.